ADVANCING EARTH AND SPACE SCIENCE

JGR Biogeosciences

RESEARCH ARTICLE
10.1029/2022JG007287

Enhancement of Summer Nitrogen Fixation by the Kuroshio Intrusion in the East China Sea and Southern Yellow Sea

Zhibing Jiang[1,2,3,4,5], Yuanli Zhu[1,3,4], Zhenhao Sun[1], Hongchang Zhai[1], Feng Zhou[5], Xiaojun Yan[6], Jiangning Zeng[1,3], Jianfang Chen[1], and Quanzhen Chen[1]

[1]Key Laboratory of Marine Ecosystem Dynamics, Second Institute of Oceanography, Ministry of Natural Resources, Hangzhou, China, [2]Key Laboratory of Ocean Space Resource Management Technology, Ministry of Natural Resource, Hangzhou, China, [3]Key Laboratory of Nearshore Engineering Environment and Ecological Security of Zhejiang Province, Hangzhou, China, [4]Observation and Research Station of Marine Ecosystem in the Yangtze River Delta, Ministry of Natural Resources, Hangzhou, China, [5]State Key Laboratory of Satellite Ocean Environment Dynamics, Second Institute of Oceanography, Ministry of Natural Resources, Hangzhou, China, [6]Marine Science and Technology College, Zhejiang Ocean University, Zhoushan, China

Key Points:

- High spatial resolution data sets of N_2 fixation rate were measured in the East China Sea and southern Yellow Sea during summer
- Summer N_2 fixation in the East China Sea was significantly enhanced by the Kuroshio intrusion, which was estimated to be 0.13–0.22 Tg N
- *Trichodesmium* and diatom-diazotroph associations were estimated to contribute largely to summer N_2 fixation in the East China Sea

Correspondence to:

Z. Jiang and Q. Chen,
jzb@sio.org.cn;
chenqz6509@126.com

Citation:

Jiang, Z., Zhu, Y., Sun, Z., Zhai, H., Zhou, F., Yan, X., et al. (2023). Enhancement of summer nitrogen fixation by the Kuroshio intrusion in the East China Sea and southern Yellow Sea. *Journal of Geophysical Research: Biogeosciences*, *128*, e2022JG007287. https://doi.org/10.1029/2022JG007287

Received 18 NOV 2022
Accepted 24 FEB 2023

Author Contributions:

Conceptualization: Zhibing Jiang, Jianfang Chen, Quanzhen Chen
Data curation: Zhibing Jiang, Hongchang Zhai, Feng Zhou, Jianfang Chen
Formal analysis: Zhibing Jiang, Yuanli Zhu, Zhenhao Sun
Funding acquisition: Zhibing Jiang, Jiangning Zeng, Jianfang Chen, Quanzhen Chen
Investigation: Zhibing Jiang, Hongchang Zhai, Feng Zhou
Methodology: Zhibing Jiang, Yuanli Zhu, Zhenhao Sun, Hongchang Zhai
Resources: Jiangning Zeng, Jianfang Chen, Quanzhen Chen
Software: Zhibing Jiang, Yuanli Zhu, Zhenhao Sun
Supervision: Jiangning Zeng, Jianfang Chen, Quanzhen Chen
Validation: Yuanli Zhu, Feng Zhou
Visualization: Yuanli Zhu, Zhenhao Sun
Writing – original draft: Zhibing Jiang

Abstract The western boundary currents are characterized by abundant diazotrophs including *Trichodesmium*, which may fuel N_2 fixation when they intrude into marginal seas. The Kuroshio, a western boundary current in the North Pacific, flows into the East China Sea (ECS) and southern Yellow Sea (SYS), which transports abundant *Trichodesmium* and diatom-diazotroph associations (DDAs). Additionally, low nitrogen:phosphorus (N:P) ratio and relatively abundant dissolved iron have been observed in the offshore ECS because of the Kuroshio intrusion as well as riverine/atmospheric inputs of P and iron. We hypothesized that the intrusion of Kuroshio greatly enhanced N_2 fixation in the ECS and SYS. N_2 fixation rates (NFRs) were measured using a $^{15}N_2$ bubble method during summer 2013. The surface and depth-integrated NFRs in the ECS and SYS were 1.45 nmol N L^{-1} d^{-1} and 81.7 μmol N m^{-2} d^{-1} on average, respectively, with the highest values of 13.84 nmol N L^{-1} d^{-1} and 511.8 μmol N m^{-2} d^{-1}. We found that NFRs were significantly higher in the ECS oceanic (Kuroshio water) and mesohaline regions (Kuroshio-affected water) than in the SYS and the ECS low-salinity and coastal upwelling regions. NFR was significantly positively correlated with the densities of *Trichodesmium* and DDAs, salinity, and temperature but was negatively with NO_3^- and N:P ratio. Generalized additive models confirmed that spatial variation in NFR was overwhelmingly contributed by *Trichodesmium* density. These findings suggested that the Kuroshio intrusion significantly enhanced N_2 fixation in the ECS through promoting growth of filamentous diazotrophs and providing appropriate nutrient environment.

Plain Language Summary Marine diazotrophs convert unbioavailable nitrogen (N_2) into bioavailable nitrogen (NH_3) through N_2 fixation, which relieves the restriction of nitrogen limitation to phytoplankton primary production and enhances oceanic carbon fixation, resulting in greater net sequestration of CO_2 and carbon sink. The western boundary currents (e.g., Kuroshio) are characterized by abundant diazotrophs including *Trichodesmium*, which may fuel N_2 fixation when they intrude into marginal seas. In order to test this hypothesis, N_2 fixation rates were measured during summer in the East China Sea (ECS) and southern Yellow Sea (SYS) influenced by the Kuroshio intrusion. We observed active N_2 fixation in the Kuroshio mainstream and affected waters in the ECS, which were characterized by abundant *Trichodesmium* and diatom-diazotroph associations, severe deficient nitrogen, and available iron and phosphorus. Nevertheless, relatively low N_2 fixation rates were detected in the SYS and the ECS low-salinity and coastal upwelling regions because of low-density filamentous diazotrophs and sufficient nitrogen. Our results revealed great enhancement of N_2 fixation by the intrusion of Kuroshio in the marginal seas. This study provided high spatial resolution data sets of N_2 fixation rate in the ECS and SYS during summer, which will be useful for understanding nitrogen and carbon biogeochemical processes.

1. Introduction

Nitrogen (N) is an essential element to phytoplankton. Although N_2 comprises a majority of the atmosphere and is abundantly dissolved in seawater, bioavailable N is deficient throughout most of the surface ocean and thereby restricts global oceanic primary production (Moore et al., 2013; Tyrrell, 1999). Marine diazotrophs convert unbioavailable N (N_2) into bioavailable N (NH_3) through N_2 fixation, which has been recognized as an important

Writing – review & editing: Jianfang Chen, Quanzhen Chen

external (new) N source in global ocean (Capone et al., 2008; Dugdale & Goering, 1967). Their fixed N relieves the restriction of N limitation to primary production in oligotrophic ocean, which enhances phytoplankton carbon (C) fixation and biological pump function, resulting in greater net sequestration of CO_2 (Falkowski, 1997; Subramaniam et al., 2008). Therefore, C sink in the ocean is largely supported by N_2 fixation. Under the visions of C neutralization and climate change (ocean warming, $p$$CO_2$ elevation, and acidification; Jiao, 2021), N_2 fixation is receiving greater interest (Hutchins et al., 2015; Jiang, Fu, et al., 2018; Zehr & Capone, 2020). However, the rates, budget, spatial distribution, and controlling factors of N_2 fixation are still highly uncertain at local, regional, and global scales (Bonnet et al., 2017; Luo et al., 2012; Tang et al., 2019; Wen et al., 2022).

The distribution, growth, and N_2 fixation of diazotrophs are generally thought to be limited by phosphorus (P) and iron (Fe) through much of the tropical and subtropical oceans (Mills et al., 2004; Sohm et al., 2011; Tanita et al., 2021; Zehr & Capone, 2020). The western boundary currents are mid-latitude, poleward-flowing, warm currents located at the western edge of ocean basin, which are characterized by high temperature, salinity, and light penetration. Because they are close to the mainland, high terrestrial inputs of P and Fe are observed therein compared with the open ocean (Jickells et al., 2005; Martiny et al., 2019), probably resulting in an alleviation of P and Fe limitation of diazotrophs (Shiozaki et al., 2014). Particularly diazotrophic cyanobacteria *Trichodesmium* (Capone et al., 1997), frequently occurs and occasionally blooms in western boundary currents, including the Gulf Stream (Palter et al., 2020), Brazil Current (Detoni et al., 2016), East Australian Current (Armbrecht et al., 2015), and Kuroshio (Jiang et al., 2019; Jiang, Li, et al., 2018; Shiozaki, Takeda, et al., 2015). Western boundary currents seem to be hotspots of marine N_2 fixation (Shiozaki et al., 2010; Tang et al., 2019). Therefore, their intrusions into marginal seas may fuel regional N_2 fixation. Emerging evidence has shown abundant diazotrophs or active N_2 fixation in subtropical-temperate seas affected by the Gulf Stream (Palter et al., 2020) and Brazil Current (Detoni et al., 2016, 2022). However, responses of diazotrophic composition and N_2 fixation to the intrusions of western boundary currents including Kuroshio remain poorly understood.

The Kuroshio, originates from the Pacific North Equatorial Current, its mainstream flows northeastward along the East China Sea (ECS) shelf break (200–1,000-m isobaths; Figure 1). Under interaction between Kuroshio and topography, the Kuroshio Surface Water (60–120 m depth) and Kuroshio Subsurface Water (120–250 m depth) intrude onto the ECS shelf from the northeast of Taiwan, forming the offshore and nearshore Kuroshio Branch Currents near 27°N, 122°E, respectively (Yang et al., 2012). During summer, the intrusion intensity of nearshore branch is strongest, which can intrude shoreward near 50-m isobath (close to Zhejiang Province) and northward to Changjiang Estuary (30.5°N) (Yang et al., 2012, 2018). In addition, Taiwan Warm Current (TWC), a mixture of the intruded Kuroshio water and the Taiwan Strait Water, flows northward and northeastward on the ECS shelf and increases appreciably during summer (approaches the southern Yellow Sea [SYS]) under prevailing southwestern monsoon (Zhou et al., 2015), resulting a remarkable upwelling along the Zhejiang coast (Lü et al., 2006). Earlier studies have indicated that summertime wind stress (particularly southwestern monsoon) plays an important role in the Kuroshio intrusion and TWC transport (Yang et al., 2018; Zhou et al., 2015). The intrusions of Kuroshio and branches bring a large amount of nutrients (particularly P) and numerous tropical species and consequently regulate ecosystem and biogeochemical processes in the ECS and SYS (ECSYS; Yang et al., 2017, 2018).

Previous studies have demonstrated that abundant diazotrophic cyanobacteria including *Trichodesmium* is transported by the Kuroshio (Cheung et al., 2019; Jiang et al., 2019; Shiozaki et al., 2018), which is widely distributed and even blooms (>1,000 trichomes L^{-1}) in the ECSYS, particularly in warm seasons (Jiang, Li, et al., 2018; Marumo & Asaoka, 1974; Shiozaki et al., 2010). In addition, severe N deficiency (N:P ratio usually <6) according to Redfield N:P ratio (16; Redfield, 1958) and relatively abundant dissolved Fe (dFe; 0.47–10.01 nmol L^{-1}) on the surface are observed in the offshore ECS (Zhang et al., 2022), because of riverine/atmospheric inputs as well as intrusion of nearshore Kuroshio Branch Current (Guo et al., 2014; Zhang et al., 2022). This intrusion across the shelf break transports a substantial amount of dFe to the broad shelf, representing natural Fe fertilization in the ECS (Zhang et al., 2022). The dFe concentrations in the ECS shelf and the adjacent Kuroshio mainstream were found to be higher than in the upstream Kuroshio of the Luzon Strait (0.25 nmol L^{-1}; Wen et al., 2022) and east of Taiwan (<0.4 nmol L^{-1}; Sato et al., 2021). Our earlier observation has revealed that the intrusions of Kuroshio and TWC promoted growth of *Trichodesmium* and diatom-diazotroph associations (DDAs; Richelia/*Calothrix*) in the ECS and even off the Changjiang Estuary (Jiang et al., 2017, 2019; Jiang, Li, et al., 2018). Such suitable macro- and micro-nutrient conditions and abundant filamentous diazotrophs may be favorable for N_2 fixation in the ECSYS. Accumulative evidence has shown much higher NFRs in the Kuroshio (up to 400 μmol N m^{-2} d^{-1};

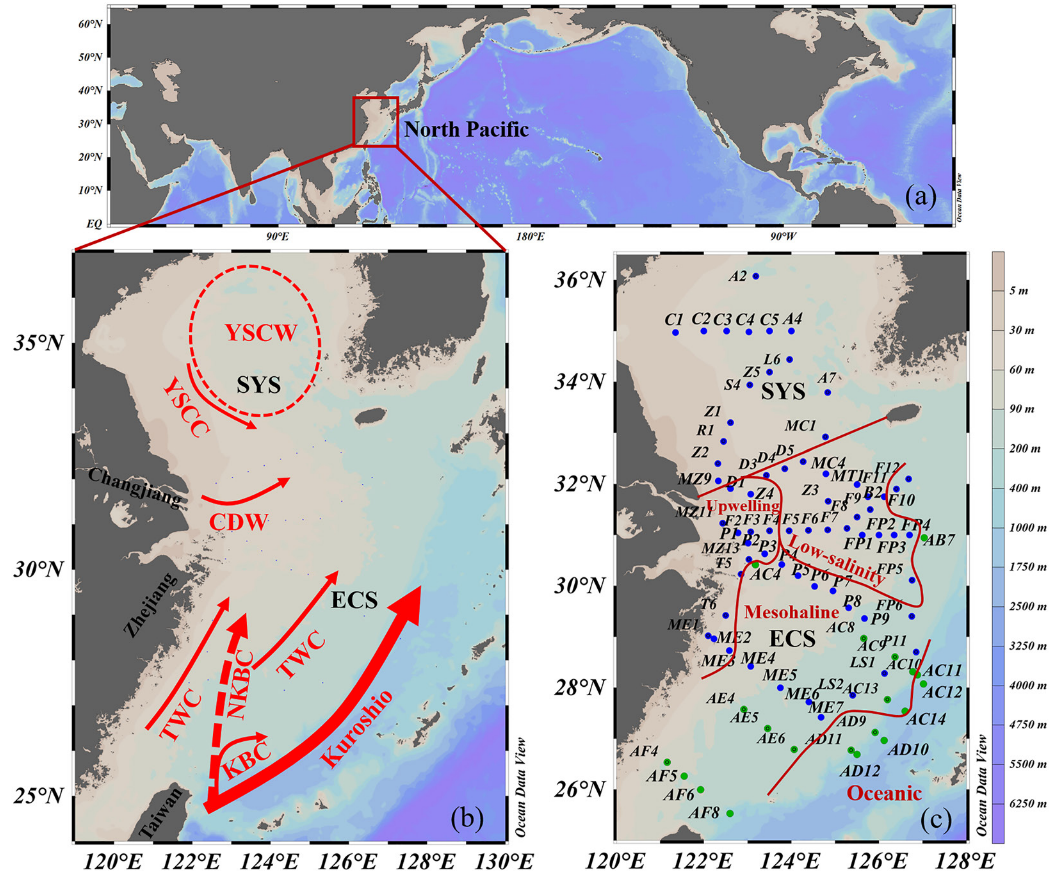

Figure 1. Schematic showing the (a) study area in the Pacific Ocean and the (b) circulation and (c) sampling stations in the East China Sea (ECS) and southern Yellow Sea (SYS) during summer (Chen, 2009; Yang et al., 2012). KBC: Kuroshio Branch Current; NKBC: nearshore Kuroshio Branch Current; TWC: Taiwan Warm Current; CDW: Changjiang Diluted Water; YSCC: Yellow Sea Coastal Current; YSCW: deeper Yellow Sea Cold Water. The ECS and SYS are divided by a dark red line from the Changjiang Estuary to Cheju Island. The ECS is divided into four regions using dark red lines, including the coastal upwelling, low-salinity (surface salinity ≤31), mesohaline (surface salinity at 31–34), and oceanic (surface salinity ≥34) regions, according to water mass distribution (Chen, 2009; Lü et al., 2006; Su & Yuan, 2005).

Shiozaki et al., 2010; Shiozaki, Takeda, et al., 2015; Wen et al., 2022) than those reported in most global seas (Luo et al., 2012; Tang et al., 2019). Therefore, N_2 fixation in the ECSYS probably contributes appreciably to regional N budget due to intrusions of Kuroshio and branches. However, direct measurements of N_2 fixation rates (NFRs) therein remain sparse and spatially limited (Shiozaki et al., 2010; Shiozaki, Takeda, et al., 2015; Wu et al., 2018; Zhang et al., 2012). Because high spatial resolution NFR data covered the entire shelf including the Kuroshio mainstream is lacking, N_2 fixation flux and controlling factors in the ECSYS remain unclear.

Although earlier work has confirmed the regulation of diazotrophic (particularly *Trichodesmium*) composition and distribution by the Kuroshio (Jiang et al., 2019; Jiang, Li, et al., 2018; Shiozaki et al., 2010; Shiozaki, Takeda, et al., 2015), influence of the Kuroshio intrusion on N_2 fixation across the entire ECSYS is still unrevealed, due to inadequate NFR data from direct measurements. We speculated that the intrusions of Kuroshio and branches (nearshore Kuroshio Branch Current and TWC) greatly enhanced summer N_2 fixation in the ECSYS through transporting abundant diazotrophic cyanobacteria and providing appropriate physicochemical environment (e.g., high temperature, severe N deficiency, and abundant dFe). Here, two interdisciplinary cruises were conducted in the ECSYS during July and August (summer) 2013. NFRs were measured using an original $^{15}N_2$ bubble method. Data of filamentous diazotrophs and physicochemical properties were obtained synchronously. Our objectives were (a) to examine the spatial distribution of NFR under the intrusion of Kuroshio, (b) to explore the controlling factors (e.g., abundance of filamentous diazotrophs, temperature, salinity, and nutrients) of N_2 fixation, and (c) to estimate local N_2 fixation budget and contribution by filamentous diazotrophs. This study addresses the inadequacy of spatial scale in NFR in the ECSYS including the Kuroshio mainstream, which contributes a more comprehensive picture of how the Kuroshio intrusion regulates N_2 fixation. In addition, our estimation of N_2 fixation flux is useful for understanding regional N biogeochemical processes and N budget.

2. Materials and Methods

2.1. Study Area and Sampling Station

During summer, the ECSYS is principally characterized by the N-limited, saline, offshore Kuroshio and TWC Water and the P-limited, fresh Changjiang Diluted Water (CDW) despite the YS Cold Water and Shelf Mixed Water (Figure 1), showing substantial spatial changes in physicochemical properties (Chen, 2009; Su & Yuan, 2005; Yang et al., 2012). The ECSYS receives a large amount of freshwater and associated nutrients (particularly N) from the Changjiang and induces the CDW to extend northeastward (Chen, 2009; Zhang et al., 2020). Therefore, the ECSYS inner shelf and Changjiang Estuary are characterized by abundant N and high N:P ratio, whereas outer shelf is N depleted (Chen, 2009; Zhang et al., 2022). The data presented here were collected from two cruises aboard the R/V *Dongfanghong* 2# during July and August 2013, which occupied a high spatial resolution across the ECSYS (Figure 1).

2.2. Data Collection

Seawater samples at each station were collected from 4 to 8 discrete depths (from surface to bottom) using 12-L Niskin bottles mounted on a SBE 917 Plus CTD rosette for analysis of nutrients, N isotopes, chlorophyll *a* (Chl-*a*), and filamentous cyanobacteria. Water depths included 2 or 3, 10, 30, 50, 75, 100, 150, 200-m depth and deep Chl-*a* maximum layer. Salinity, temperature, depth, and turbidity were measured in situ. Mixed-layer depth (MLD) was defined as the depth where density (σ_t; derived from salinity, temperature, and pressure) was higher 0.125 kg m^{-3} than that on the surface (Huang & Russell, 1994). NO_3^- and dissolved reactive phosphorus (DRP) were measured using a continuous-flow analyzer (Skalar San^{++}). Water samples (100–250 mL) for Chl-*a* analysis were filtered onto 0.7-μm GF/F filters using low cacuum pressure. After extraction in 90% acetone for 24 hr at −20°C Chl-*a* concentrations were analyzed using a Turner Design Fluorometer. Water samples (1,000 mL) of filamentous cyanobacteria were fixed with glutaraldehyde to a final concentration of 2%. Colonial and free trichomes of *Trichodesmium* and *Richelia/Calothrix* heterocysts (symbiotic with *Hemiaulus*, *Rhizosolenia/Guinardia*, and *Chaetoceros/Bacteriastrum*) were enumerated on a 1-mL scaled slide using a fluorescence microscope (Leica DM3000B). Depth-integrated densities (DIDs) of their trichomes or heterocysts were calculated using trapezoidal integration over the sampling depths. Partial data on salinity, temperature, turbidity, nutrients, Chl-*a*, and filamentous cyanobacteria were derived from previous studies (Jiang et al., 2019; Zhang et al., 2022).

Seawater for the NFR incubation experiment was sampled from three depths that corresponded to 100%, 10%, and 1% of surface irradiance using Niskin bottles, according to the PAR in the water column. NFRs were determined using the $^{15}N_2$ incorporation technique (Montoya et al., 1996; Zhang et al., 2012). Briefly, duplicate water samples were filled bubble free into 580-mL transparent glass bottles. After filling, 1 mL $^{15}N_2$ (99 at% ^{15}N, Cambridge Isotope Laboratories) was spiked with a septum using a gastight syringe (Agilent), with the pressure across the septum balanced by another syringe. Each bottle was gently shaken for several minutes before incubation. Incubations were performed in flow-through deck-board incubators and were covered with neutral-density screens to adjust light densities (100%, 10%, and 1% of natural sea-surface irradiance). After 24-hr incubation, N_2 fixation samples were filtered under gentle vacuum through a precombusted (4 hr at 450°C) Whatman GF/F filter membrane and then were immediately stored at −20°C. Natural ^{15}N abundance in particulate organic N (PON) was measured for calculating the ^{15}N enrichment during incubation. At the land laboratory, the filters for PON and ^{15}N measurements were dried at 60°C and pelletized in tin capsules. The PON concentration and ^{15}N abundance (δ^{15}N; ‰) were measured using a Flash 2000 elemental analyzer coupled to a isotope ratio mass spectrometer. The NFRs and their detection limits (minimum quantifiable rates; 0.01–1.64 nmol N L^{-1} d^{-1}) were calculated following Montoya et al. (1996). Depth-integrated NFR at each station was calculated by trapezoidal integration over the sampling depths in the euphotic zone (1% of surface PAR). The present incubation experiment (original $^{15}N_2$ bubble method) might underestimate the NFR, because the injected gas bubble was not likely to attain equilibrium with the surrounding water during the incubation period and results in a lower actual $^{15}N_2$ concentration than theoretically calculated (Mohr et al., 2010). However, the level of underestimation of the bubble method is thought to be low in *Trichodesmium*-dominant waters because *Trichodesmium* can float to the

Table 1
Regional Differences of Environmental Variables in the ECS and SYS (ECSYS) by Using Kruskal–Wallis (H) Test

Parameters	ECS coastal upwelling region (n = 16)	ECS low-salinity region (n = 18)	ECS mesohaline region (n = 30)	ECS oceanic region (n = 6)	SYS (n = 16)	H
Surface salinity	32.2 ± 1.4^{c}	29.2 ± 0.8^{a}	33.2 ± 0.8^{d}	34.2 ± 0.1^{e}	30.5 ± 0.7^{b}	66.7***
Surface temperature (°C)	23.9 ± 1.8^{a}	27.3 ± 0.7^{b}	28.6 ± 0.8^{c}	29.4 ± 0.8^{d}	24.5 ± 1.2^{a}	68.9***
Integration depth (m)	39 ± 16^{a}	61 ± 17^{b}	113 ± 48^{c}	195 ± 12^{d}	59 ± 23^{b}	52.9***
MLD (m)	8.1 ± 3.6^{a}	13.3 ± 4.6^{bc}	18.2 ± 9.5^{c}	44.0 ± 21.5^{d}	11.9 ± 3.2^{b}	34.0***
Surface turbidity (NTU)	2.77 ± 3.79^{d}	0.19 ± 0.14^{c}	0.10 ± 0.08^{b}	0.02 ± 0.01^{a}	0.62 ± 1.10^{c}	50.7***
Surface NO_3^- (μmol L^{-1})	12.61 ± 8.67^{c}	2.64 ± 3.03^{b}	0.35 ± 1.05^{a}	0.06 ± 0.07^{a}	2.03 ± 4.57^{a}	44.0***
Surface DRP (μmol L^{-1})	0.66 ± 0.44^{b}	0.13 ± 0.03^{a}	0.24 ± 0.21^{a}	0.13 ± 0.08^{a}	0.17 ± 0.06^{a}	26.8***
Surface NO_3^-/DRP ratio	21.9 ± 16.9^{b}	19.9 ± 20.6^{b}	1.5 ± 2.6^{a}	0.8 ± 0.9^{a}	8.2 ± 13.7^{a}	41.4***
Surface Chl-*a* (mg m^{-3})	6.34 ± 7.56^{d}	1.79 ± 2.22^{c}	0.33 ± 0.41^{b}	0.08 ± 0.05^{a}	3.54 ± 5.06^{c}	53.3***

Note. Low-salinity: salinity ≤31; mesohaline: 31 < salinity <34; oceanic: salinity ≥34. MLD: Mixed-layer depth; DRP: dissolved reactive phosphorus; Chl-*a*: chlorophyll *a*. Superscripted lower-case letters within the same row indicate significant ($p < 0.05$) difference. ***$p < 0.001$.

top of the bottle and directly use the added $^{15}N_2$ gas (Großkopf et al., 2012). Since *Trichodesmium* is abundant in the ECSYS (Jiang et al., 2019; Jiang, Li, et al., 2018), particularly in the Kuroshio mainstream and affected waters (Jiang, Li, et al., 2018; Marumo & Asaoka, 1974; Shiozaki, Takeda, et al., 2015), the magnitude of underestimation of the bubble method performed in our study area was likely low. Regardless, our data remains useful to reveal spatial distribution of N_2 fixation in the ECSYS and is comparable with the earlier results in Kuroshio and adjacent seas.

2.3. Data Analysis

To clarify influence of saline Kuroshio intrusion on NFR and associated filamentous cyanobacteria and physicochemical variables, the ECS was divided into four regions, including the coastal upwelling, low-salinity (surface salinity ≤31; mainly controlled by the CDW), mesohaline (surface salinity at 31–34, mainly influenced by the TWC and nearshore Kuroshio Branch Current), and oceanic (surface salinity ≥34; the Kuroshio mainstream) regions (Figure 1). These four regions of the ECS were divided according to the thermohaline properties of different water masses (Chen, 2009; Lü et al., 2006; Su & Yuan, 2005). SPSS 20.0 was used for data analysis. A Kruskal–Wallis one-way analysis of variance was used to test for significant ($p < 0.05$) differences in environmental variables, *Trichodesmium* and *Richelia/Calothrix* densities, and NFRs among regions because most variables failed to satisfy the assumptions of normality using Kolmogorov–Smirnov test and homogeneity using Levene's test. Kruskal–Wallis test statistic (H value) is a measure of the observed spread of rank average, which is highly associated with the significance of regional difference for each variable. Relationship between NFRs and environmental variables and DIDs of filamentous diazotrophs was conducted using Spearman's rank correlation or regression analysis. Generalized additive models (GAMs) were used to estimate the relative contribution of environmental variables (temperature, salinity, MLD, turbidity, and nutrients) and densities of *Trichodesmium* and DDAs to variations in surface and depth-integrated NFRs using *R* software. GAMs were established using the mgcViz package (version 4.0.2). Model building used a forward stepwise approach with the greatest cumulative explained deviation. The model with the lowest Akaike information criterion value and greatest adjusted R^2 was selected as the optimal model. ODV 4 was used to depict the spatial distribution of NFR, filamentous diazotrophic density, and environmental variables.

3. Results

3.1. Environmental Parameters

The physicochemical parameters differed significantly ($p < 0.001$) among regions of the ECSYS divided according to surface salinity distribution (Table 1). Surface salinity was markedly low (≤31) off the Changjiang Estuary and was high in the ECS open waters, because of the CDW extension and the strong intrusions of nearshore

10.1029/2022JG007287

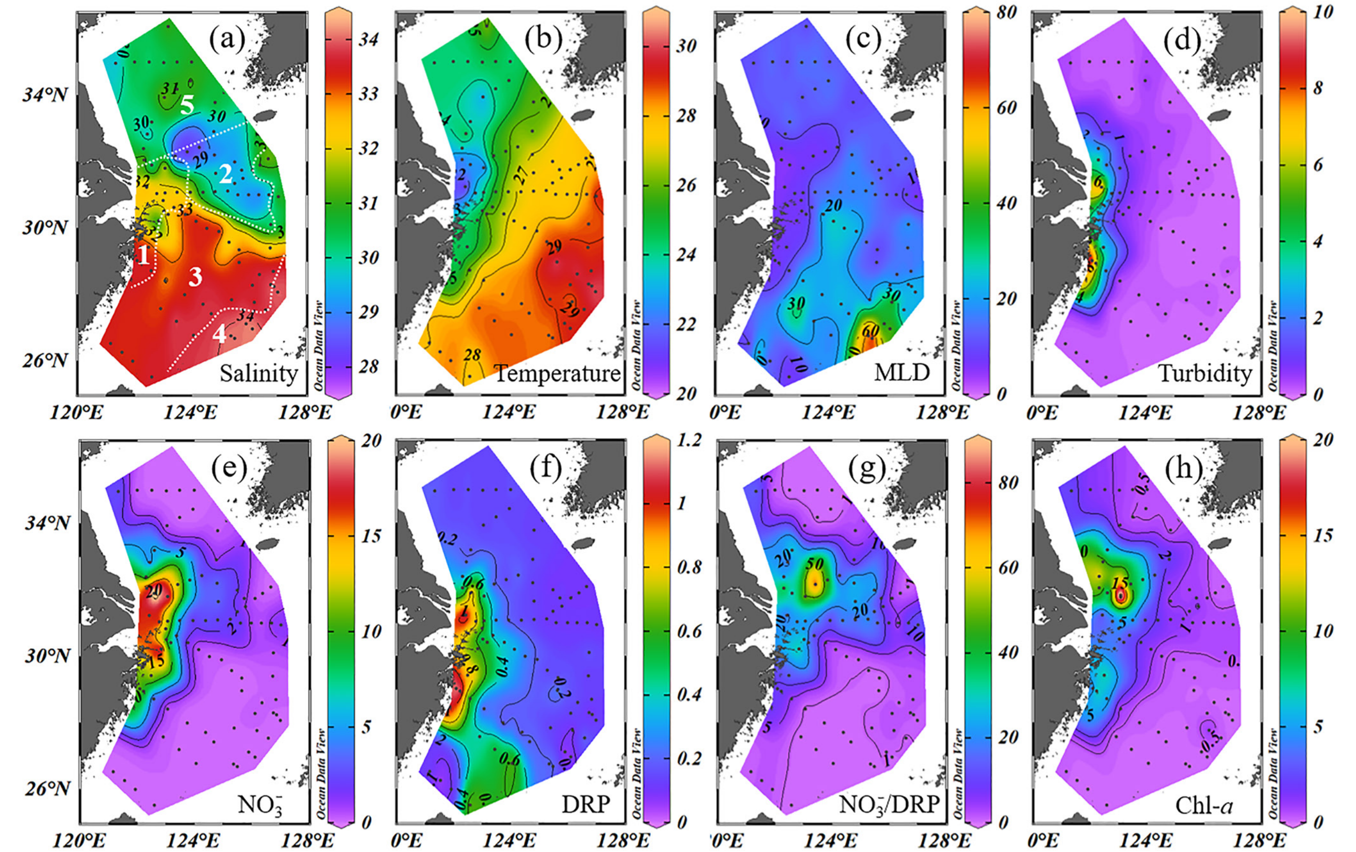

Figure 2. Environmental parameters (except MLD) on the surface in the ECSYS. (a) salinity, the dashed polygons 1, 2, 3, 4, and 5 (white Arabic numerals) indicate the coastal upwelling, low-salinity, mesohaline, and oceanic regions of the ECS and the SYS, respectively; (b) temperature (°C); (c) turbidity (NTU); (d) mixed-layer depth (MLD; m); (e) NO_3^- (μmol L^{-1}); (f) dissolved reactive phosphorus (DRP; μmol L^{-1}); (g) NO_3^-/DRP ratio; (h) chlorophyll *a* (Chl-*a*; mg m^{-3}).

Kuroshio Branch Current and TWC (Figure 2a). The ECS oceanic region was characterized by the Kuroshio mainstream with average surface salinity of 34.2 ± 0.1. The ECS mesohaline region was influenced by the nearshore Kuroshio Branch Current and TWC with average surface salinity of 33.2 ± 0.8. Surface temperature showed significantly ($p < 0.05$) lower in the SYS (24.5 ± 1.2°C) and the ECS coastal region (27.3 ± 0.7°C) than in the ECS oceanic (29.4 ± 0.8°C) and mesohaline (28.6 ± 0.8°C) regions (Figure 2b). Additionally, obvious upwelling with low temperature (23.9 ± 1.8°C) and high salinity (32.2 ± 1.4) was observed on the surface in the ECS coastal waters, because of shoreward intrusion of deeper TWC and modified nearshore Kuroshio Branch Current. MLD was high in the Kuroshio mainstream (up to 78 m) and on the middle ECS shelf (Figure 2c), which was consistent with the intrusion of nearshore Kuroshio Branch Current. The turbidity decreased obviously from the inshore (>10 NTU) to offshore (<0.1 NTU; Figure 2d). The MLD, integration depth, and surface salinity and temperature were significantly ($p < 0.05$) higher in the ECS oceanic and mesohaline regions than in the ECS coastal upwelling and low-salinity regions and in the SYS (Table 1). However, turbidity showed opposite regional distribution.

The surface concentrations of NO_3^- (>10 μmol L^{-1}; Figure 2e) and DPR (>1 μmol L^{-1}; Figure 2f) were markedly high in the Changjiang Estuary and coastal upwelling waters but low in the ECS oceanic waters (due to oligotrophic Kuroshio) and in the central part of the SYS (due to strong stratification caused by deeper YS Cold Water). Particularly in the Kuroshio mainstream, NO_3^- concentrations were undetectable at most stations. DRP concentration was relatively high (>0.4 μmol L^{-1}) from the northeast of Taiwan to Zhejiang coastal upwelling waters and the Changjiang Estuary, indicating important sources of DRP from Changjiang and intrusion of nearshore Kuroshio Branch Current. The distribution of NO_3^-/DRP ratio was consistent with distribution of NO_3^- concentration, which showed higher value in the Changjiang Estuary (up to 85) than in the ECS oceanic waters and in the central part of SYS (Figure 2g). Chl-*a* concentrations were higher in the Changjiang Estuary and coastal upwelling waters (>2 mg m^{-3}) than in the ECS oceanic waters (usually <0.2 mg m^{-3}) and in the central part of the SYS (≤0.6 mg m^{-3}). The concentrations of NO_3^-, DRP, and Chl-*a* and NO_3^-/DRP ratio were significantly ($p < 0.05$) higher in the ECS coastal upwelling and low-salinity region than in the ECS oceanic and mesohaline regions and in the SYS (Table 1).

3.2. Filamentous Cyanobacteria Density

The trichome of *Trichodesmium* in the ECSYS included colonial and free forms. The average colonial and free trichomes on the surface in the ECSYS were 77.0 and 95.5 trichomes L^{-1}, respectively, whereas the average colonial and free trichomes in the water column were 3,359 × 10^3 and 5,118 × 10^3 trichomes m^{-2}. The colony was usually found in the ECS mesohaline and oceanic regions, particularly in the Kuroshio mainstream with the highest density of 2,083 trichomes L^{-1} on the surface and of 65.20 × 10^6 trichomes m^{-2} in the euphotic zone (Figure 3). The highest surface density (1,275 trichomes L^{-1}) and DID (74.10 × 10^6 trichomes m^{-2}) of free trichomes was also found therein. However, free trichomes were widely distributed across the entire ECSYS, although DID (4.1 × 10^3 trichomes m^{-2}) in the SYS was extremely low. Figure 3 showed that *Trichodesmium* density on the surface (≤3,358 trichomes L^{-1}) and in the water column (≤121 × 10^6 trichomes m^{-2}) decreased from the southeast to the north and the northwest along the intrusion path of nearshore Kuroshio Branch Current. Both the colonial and free trichomes of *Trichodesmium* were significantly ($p < 0.05$) higher in the ECS oceanic and mesohaline regions than in the SYS and in the ECS low-salinity and upwelling regions (Figure 3).

DDAs in the ECSYS included *Richelia* and *Calothrix*. *Richelia* symbioses inside the cells of host diatoms *Hemiaulus*, *Rhizosolenia*, and *Guinardia*, whereas *Calothrix* attached epiphytically to host diatoms *Chaetoceros* and *Bacteriastrum*. DDAs were not detected in the SYS. The average surface density and DID of *Richelia/Calothrix* in the ECS were 16.3 heterocysts L^{-1} and 2160 × 10^3 heterocysts m^{-2}, respectively, with the highest surface density of 252.1 heterocysts L^{-1} and DID of 25.74 × 10^6 heterocysts m^{-2}. *Richelia/Calothrix* DIDs were significantly ($p < 0.05$) higher in oceanic and mesohaline regions than in coastal upwelling and low-salinity regions (Figure 3).

3.3. N_2 Fixation Rate (NFR)

The average depth-integrated NFRs in the euphotic zone in the ECSYS ranged from undetectable to 511.8 μmol N m^{-2} d^{-1}, averaged at 81.7 ± 151.2 μmol N m^{-2} d^{-1} ($n = 29$). The surface NFRs ranged from undetectable to 13.84 nmol N L^{-1} d^{-1}, averaged at 1.45 ± 2.71 nmol N L^{-1} d^{-1} ($n = 39$). NFRs were undetected at several stations (e.g., P1 and T5) in the ECS low-salinity and coastal upwelling regions. Figure 4 showed high NFR in the southeastern ECS but low in the Changjiang Estuary and ECS coastal waters. The depth-integrated NFR was significantly ($p < 0.05$) higher in the ECS oceanic region than in the SYS and in the ECS mesohaline, low-salinity, and coastal upwelling regions, which averaged at 428.3, 11.2, 47.8, 9.2, and 2.8 μmol N m^{-2} d^{-1}, respectively (Figure 4c). The surface NFRs among regions showed similar spatial variation (Figure 4d). The average NFRs ($n = 29$) based on water column measurements under 100%, 10%, and 1% of natural surface irradiance were 1.74 ± 3.09, 1.54 ± 2.67, and 0.38 ± 0.34 nmol N L^{-1} d^{-1}, respectively (Table 2).

3.4. Relationship Between NFR and Filamentous Diazotrophs and Physicochemical Factors

Spearman's correlation showed that the depth-integrated and surface NFRs in the ECSYS were significantly ($p < 0.05$) positively correlated with surface temperature and salinity and MLD but was negatively with surface turbidity, NO_3^-, DRP, NO_3^-/DRP ratio, and Chl-*a*. Figure 5 showed that both the surface and depth-integrated NFRs were markedly higher in the Kuroshio Surface Water (Kuroshio mainstream; temperature ≥28°C and salinity ≥34) and TWC Water (mixing with the intrusion of nearshore Kuroshio Branch Current; temperature ≥28°C and salinity: 32–34) than in the CDW (salinity ≤31), Shelf Mixed Water, and upwelling water (temperature <26.5°C; salinity ≥31.5). The Shelf Mixed Water can be considered a mixture of coastal water with nearshore Kuroshio Branch Current Water and TWC Water. Regression analysis showed that the depth-integrated and surface NFRs were significantly ($p < 0.001$) positively correlated with densities of *Trichodesmium* and *Richelia/Calothrix*. Table 3 showed results of GAMs with the least Akaike information criterion values and the best fit (greatest adjusted R^2 and cumulative explained deviation). *Trichodesmium* density explained (97%) more variations in the depth-integrated and surface NFRs than environmental parameters and *Richelia/Calothrix* density. However, MLD, integration depth, salinity, and DRP contributed significantly ($p < 0.05$) to depth-integrated NFR variation and MLD contributed significantly ($p < 0.05$) to surface NFR variation.

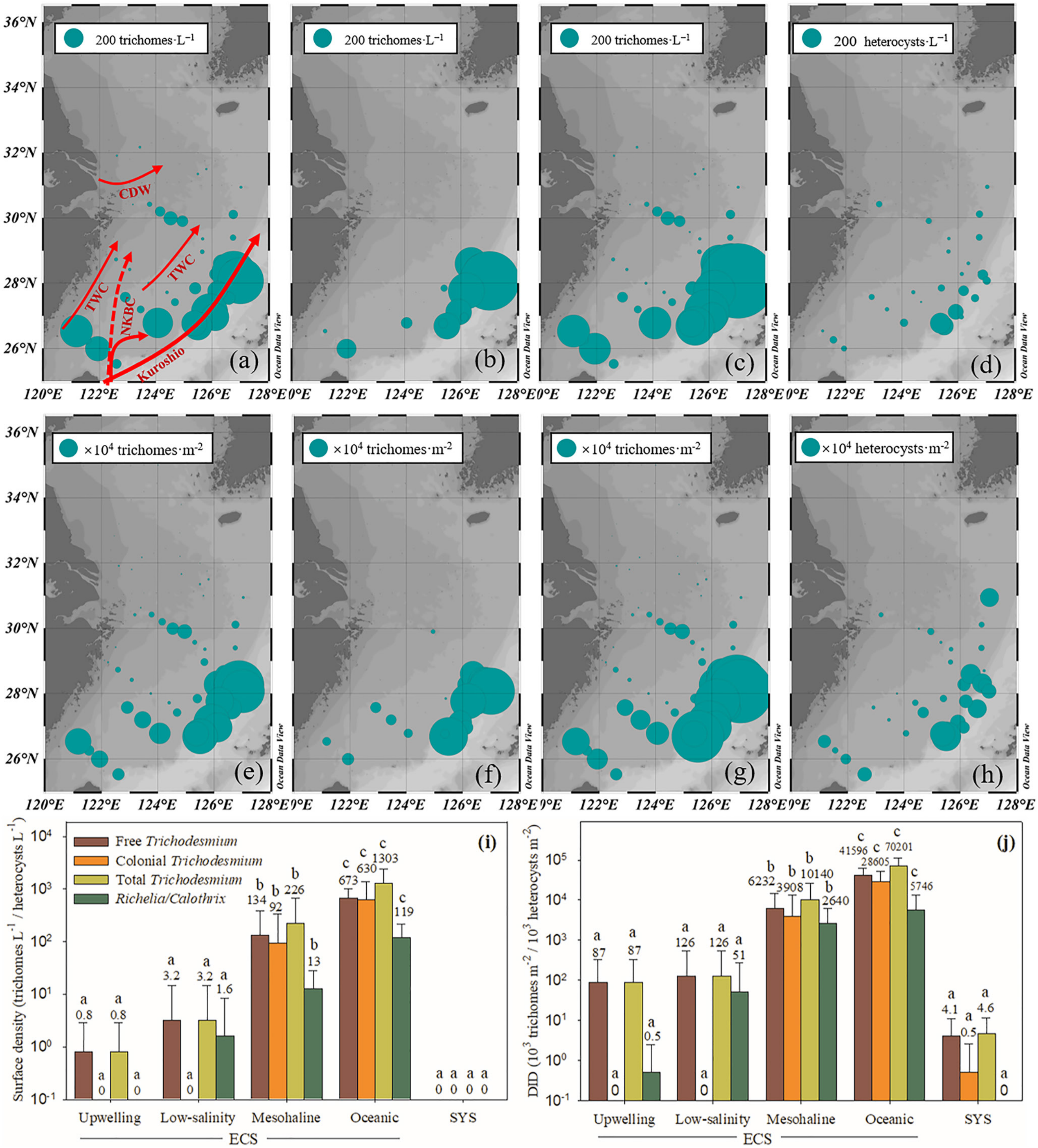

Figure 3. Surface densities and depth-integrated densities (DIDs) of *Trichodesmium* and diatom-diazotroph associations (DDAs; *Richelia/Calothrix*) in the ECSYS. (a and e) free *Trichodesmium*; (b and f) colonial *Trichodesmium*; (c and g) total *Trichodesmium*; (d and h) total heterocysts; (i) surface densities in different regions; (j) DIDs in different regions. Numbers on the bar plots indicate regional average values of surface densities and DIDs; lower-case letters on the bar plots indicate significant ($p < 0.05$) difference in densities and DIDs among regions.

10.1029/2022JG007287

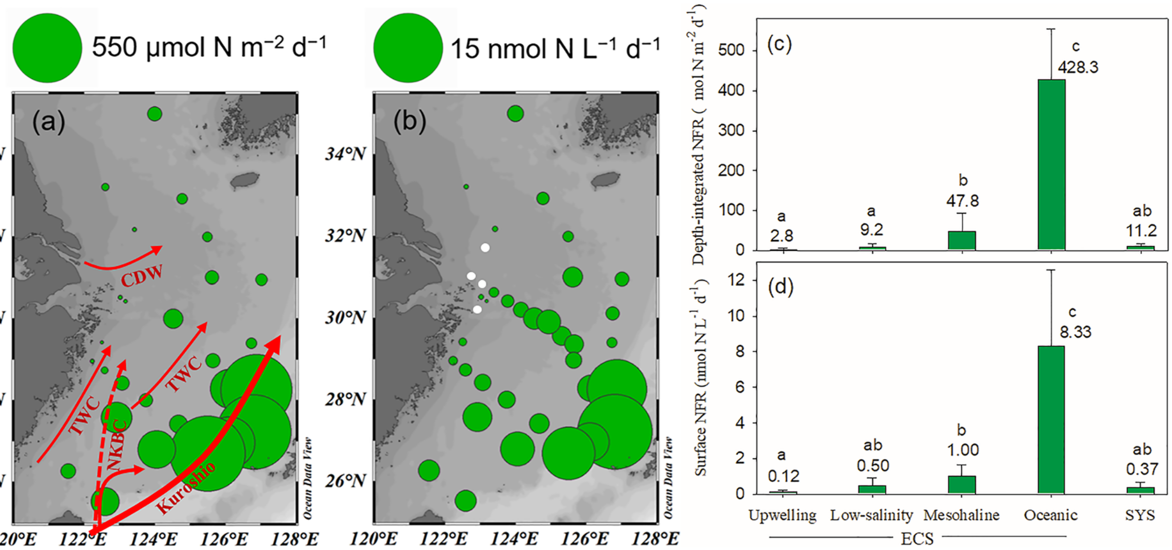

Figure 4. Depth-integrated (μmol N m^{-2} d^{-1}) and surface (nmol N L^{-1} d^{-1}) N_2 fixation rates (NFRs) in the ECSYS. (a) spatial distribution of depth-integrated NFR; (b) spatial distribution of surface NFR; (c) depth-integrated NFRs among regions; (d) surface NFRs among regions. White circles indicate undetectable NFRs at stations P1, P2, T5, and Z4; numbers on the bar plots indicate regional average values of depth-integrated and surface NFRs; lower-case letters on the bar plots indicate significant ($p < 0.05$) difference in depth-integrated and surface NFRs among regions.

4. Discussion

4.1. Enhancement of N_2 Fixation by the Kuroshio Intrusion

The depth-integrated NFR was significantly ($p < 0.05$) higher in the ECS oceanic region (Kuroshio mainstream; 428.3 μmol N m^{-2} d^{-1}) than in other regions of the ECS and in the SYS (Figure 4c). Zhang et al. (2012) also found much higher NFR in the Kuroshio mainstream (221 μmol N m^{-2} d^{-1}) than on the ECS shelf (21 μmol N m^{-2} d^{-1}). Figure 6 showed that surface and depth-integrated NFRs were significantly ($p < 0.001$) positively correlated with densities of *Trichodesmium* and DDAs (*Richelia/Calothrix*). Shiozaki, Takeda, et al. (2015) found similar correlation between NFR and *Trichodesmium* density in the Kuroshio and the neighboring ECS (near Japan). Because the N_2 fixation efficiency of colonial trichomes of *Trichodesmium* was much higher than that of free trichomes (Letelier & Karl, 1998; Saino & Hattori, 1982), the high density and colonial contribution of *Trichodesmium* in the Kuroshio supported active N_2 fixation therein. Result of GAMs showed that spatial variation of NFRs was overwhelmingly (97%) contributed by *Trichodesmium* density (Table 3). Apparently, spatial distribution of NFR in the ECSYS was considerably determined by composition and density of filamentous diazotrophs.

The present NFRs in the ECS low-salinity (9.2 μmol N m^{-2} d^{-1}) and upwelling (2.8 μmol N m^{-2} d^{-1}) regions (Figure 4c) were consistent with previous measurement (7.8 μmol N m^{-2} d^{-1}) in the ECS low-salinity region (Zhang et al., 2012). However, our NFR (11.2 μmol N m^{-2} d^{-1}) in the SYS was much lower than previously measured across the central part of the SYS (104 μmol N m^{-2} d^{-1}) by Zhang et al. (2012). Such inconsistence was probably attributed to the different water masses and associated nutrient conditions in the SYS. The central part of the SYS was controlled by deeper YS Cold Water and formed a strong thermocline, which prevented upwards delivery of nutrients and resulted in depletion of NO_3^- and extremely low NO_3^-/DRP (Figures 2e and 2g). However, our measured stations were mainly situated in the southern part of the SYS where nutrient conditions

Table 2
Spearman's Correlation Coefficient (r) of NFRs and Surface Environmental Variables (Except MLD) in the ECSYS

Parameters	Temperature	Salinity	MLD	Turbidity	NO_3^-	DRP	NO_3^-/DRP	Chl-*a*
Surface NFR	0.67***	0.64***	0.71***	−0.81***	−0.71***	−0.36*	−0.67***	−0.83***
Depth-integrated NFR	0.74**	0.70***	0.78***	−0.86***	−0.80***	−0.38*	−0.75***	−0.88***

Note. *$p < 0.05$; **$p < 0.01$; ***$p < 0.001$.

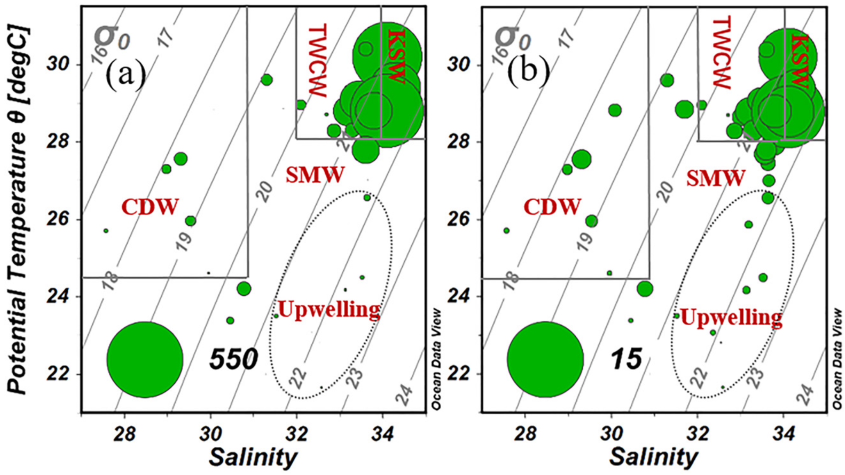

Figure 5. Diagram of (a) depth-integrated N_2 fixation rate (NFR) (μmol N m^{-2} d^{-1}) and (b) surface NFR (nmol N L^{-1} d^{-1}) versus temperature–salinity (water masses) in the ECSYS. Different surface water masses were determined by the salinity and temperature properties (Chen, 2009; Lü et al., 2006; Su & Yuan, 2005). TWCW: Taiwan Warm Current Water; KSW: Kuroshio Surface Water; SMW: Shelf Mixed Water. The biggest green circles with the numbers 550 and 15 placed in lower left quarters indicate values of depth-integrated and surface NFRs, respectively.

(NO_3^- repletion) were unfavorable for N_2 fixation because of extension of eutrophic CDW (Figure 2). *Trichodesmium* density was considerably lower in the SYS than in the ECS (Figures 3i and 3j). Our investigation in 2011 found similar pattern (Jiang, Li, et al., 2018). Moreover, *Richelia/Calothrix* was undetectable in the SYS. We speculated that unicellular cyanobacteria or noncyanobacteria diazotrophs (e.g., proteobacteria) might be responsible for a major portion of N_2 fixation in the temperate SYS. Zhang, Song, et al. (2015) demonstrated that heterotrophic diazotrophs (Gammaproteobacteria) were dominant in the SYS using real-time PCR and clone library analysis of *nifH* genes. Shiozaki, Nagata, et al. (2015) found high summer NFRs (up to 13.6 nmol N L^{-1} d^{-1}) in the temperate coastal region of Japan, largely contributed by unicellular cyanobacteria. These studies supported our speculation.

The present NFR (89.8 μmol N m^{-2} d^{-1}) in the ECS was higher than that previously reported (41 μmol N m^{-2} d^{-1}) by Zhang et al. (2012). Our station number of high NFR was much more than previously measured in oceanic (4 vs. 1) and mesohaline regions (12 vs. 7), which increased the present average NFR across the ECS. The present surface NFR (8.33 ± 4.25 nmol N L^{-1} d^{-1}) in the Kuroshio mainstream was slightly higher than those measured previously using original $^{15}N_2$ bubble method (3.55 and 4.63 nmol N L^{-1} d^{-1}, respectively; Shiozaki, Takeda,

Table 3
Results of Generalized Additive Models Between NFRs (Surface and Depth-Integrated) and Environmental Variables and Densities (Surface and Depth-Integrated) of Trichodesmium and DDAs in the ECSYS

NFR	Variables	Adjusted R^2	CED	AIC
Depth-integrated NFR	*Trichodesmium****	0.965	96.8%	280.6
	*Trichodesmium**** + MLD***	0.989	99.1%	249.0
	*Trichodesmium**** + MLD*** + ID ***	0.994	99.5%	230.6
	*Trichodesmium**** + MLD*** + ID*** + DDAs**	0.996	99.7%	221.9
	*Trichodesmium**** + MLD*** + ID*** + DDAs* + Salinity	0.996	99.8%	222.8
	*Trichodesmium**** + MLD** + ID** + DDAs + Salinity + Chl-*a*	0.996	99.8%	222.3
	*Trichodesmium**** + MLD*** + ID*** + DDAs + Salinity* + Chl-*a* + DRP*	0.997	99.8%	216.7
Surface NFR	*Trichodesmium****	0.970	97.2%	57.1
	*Trichodesmium**** + MLD***	0.977	97.9%	47.5
	*Trichodesmium**** + MLD** + Temperature	0.979	98.1%	45.1

Note. CED: cumulative explained deviation; AIC: Akaike information criterion. ID: integration depth. *$p < 0.05$; **$p < 0.01$; ***$p < 0.001$.

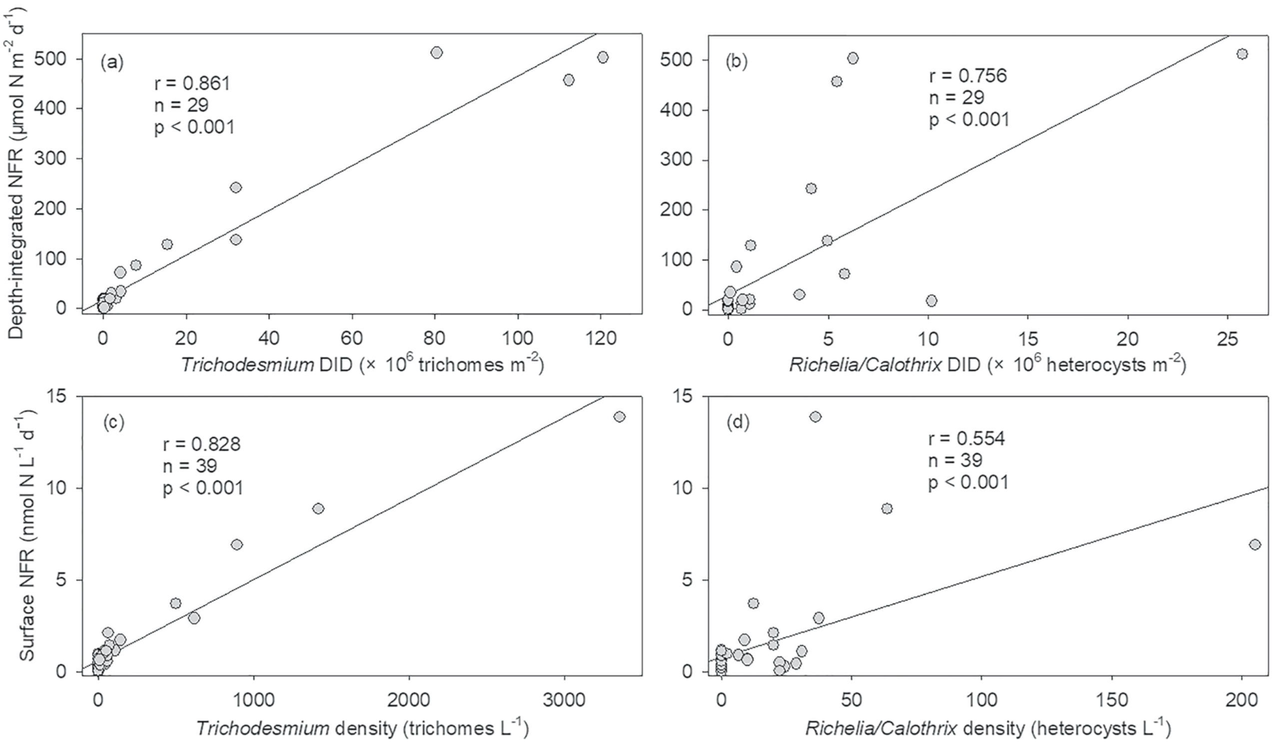

Figure 6. Regression between N_2 fixation rates (NFRs) and densities of *Trichodesmium* and *Richelia/Calothrix* in the ECSYS.

et al., 2015; Zhang et al., 2012) and acetylene reduction assay (4.12 nmol N L^{-1} d^{-1}; Wu et al., 2018). Also, this rate was consistent with those (6–18 nmol N L^{-1} d^{-1}) measured in and near the Gulf Stream of the North Atlantic subtropical gyre using modified $^{15}N_2$ bubble method (Palter et al., 2020). However, our present depth-integrated NFR in the Kuroshio mainstream (428 ± 127 μmol N m^{-2} d^{-1}) was much higher than those previously measured in the upstream Kuroshio (180.5 ± 34.3 μmol N m^{-2} d^{-1}; Chen et al., 2014) and the ECS Kuroshio mainstream and adjacent waters near Japan (181–232 μmol N m^{-2} d^{-1}; Shiozaki et al., 2010; Shiozaki, Takeda, et al., 2015) during summer using original bubble method, which might be attributed to appreciably high densities of filamentous diazotrophs during our investigation. These high surface and depth-integrated NFRs in the Kuroshio mainstream were much lower than those (62 nmol N L^{-1} d^{-1} and 753 μmol N m^{-2} d^{-1}) measured around the Miyako Islands in September 2009 when *Trichodesmium* bloomed with an extremely high density (>20,000 trichomes L^{-1}; Shiozaki, Takeda, et al., 2015). The depth-integrated NFR in the ECS was also much higher than those reported in the South China Sea (Chen et al., 2014; Voss et al., 2006; Wen et al., 2022; Zhang, Chen et al., 2015), Philippine Sea (Shiozaki, Takeda, et al., 2015), and western and central North Pacific (Shiozaki et al., 2010; Zhang et al., 2019), which have been characterized by low density of *Trichodesmium* under limitation of Fe or P (Sohm et al., 2011; Tanita et al., 2021). Table 3 showed that DRP contributed significantly ($p < 0.05$) to depth-integrated NFR variation in the ECSYS, indicating important regulation of DRP on N_2 fixation. Although NFRs in the entire ECS coincided with those reported in most seas worldwide (Luo et al., 2012; Tang et al., 2019), our data measured in the Kuroshio mainstream was relatively high.

In addition to filamentous diazotrophs, water mass variation associated temperature, salinity, nutrients, and light profoundly influenced N_2 fixation in the ECSYS. The NFRs in the N-depleted, clear, warm, saline Kuroshio and TWC water were considerably higher than those in the N-replete, turbid, cold or fresh CDW, YS Cold Water, and Shelf Mixed Water (Figure 5). Table 2 affirmed that the NFR was significantly ($p < 0.001$) positively correlated with temperature and salinity but was negatively with NO_3^-, NO_3^-/DRP, and turbidity. Laboratory experiments showed that salinity and temperature for optimal growth and N_2 fixation of *Trichodesmium* ranged from 33 to 37 (Fu & Bell, 2003) and 24–30°C (Breitbarth et al., 2007). As described previously, warm and saline environments in the ECS were favored by *Trichodesmium* and *Richelia/Calothrix* (Jiang et al., 2019). Our results clearly revealed relatively depleted NO_3^- but replete DRP associated with the intrusion path of nearshore Kuroshio

Branch Current from the northeast of Taiwan to the Zhejiang coastal waters (Figure 2f), being highly consistent with active N_2 fixation therein (Figure 4). The dFe concentration measured simultaneously in the ECS Kuroshio mainstream (0.8 nmol L^{-1}; Zhang et al., 2022) was much higher than those in the upstream Kuroshio of the Luzon Strait (0.25 nmol L^{-1}; Wen et al., 2022) and east of Taiwan (<0.4 nmol L^{-1}; Sato et al., 2021), because of large inputs of trace elements from rivers, atmospheric deposition, Taiwan Strait Water, and Kuroshio intrusion (Guo et al., 2014; Zhang et al., 2022). Therefore, high temperature, deficient N, extremely low NO_3^-/DRP, and abundant dFe were conducive to N_2 fixation in oceanic and mesohaline waters of the ECS influenced by the Kuroshio. It is well recognized that bioavailable Fe and P are limited N_2 fixation in most oceanic warm regions (Mills et al., 2004; Sohm et al., 2011; Tanita et al., 2021). The relatively high concentrations of dFe and DRP may be the crucial factors for active N_2 fixation in the ECS Kuroshio mainstream where was thought to be hotspot of N_2 fixation worldwide (Shiozaki et al., 2010; Shiozaki, Takeda, et al., 2015).

Previous studies have indicated that abundant *Trichodesmium* and Richelia/*Calothrix* are transported by the intrusions of Kuroshio and TWC into the ECSYS (Cheung et al., 2019; Jiang et al., 2019; Jiang, Li, et al., 2018; Marumo & Asaoka, 1974; Shiozaki, Takeda, et al., 2015). Moreover, suitable physicochemical properties (nutrients, temperature, and light penetration) in the Kuroshio mainstream and affected waters promote growth of diazotrophs (particularly *Trichodesmium*) and consequent N_2 fixation in the offshore ECS (Jiang et al., 2019; Jiang, Li, et al., 2018; Zhang et al., 2012). Figures 3 and 4 confirmed shoreward and northward decreasing trends of filamentous diazotrophic density and NFR from the Kuroshio to the ECS coast and SYS. These findings suggested great enhancement of N_2 fixation by the Kuroshio intrusion in the ECSYS. Lu et al. (2019) also found that the transportation of *Trichodesmium* by the Kuroshio intrusion significantly increased *Trichodesmium* density and NFR in the northern South China Sea. Similar results were observed in other western boundary currents, including the Gulf Stream (Palter et al., 2020), East Australian Current (Armbrecht et al., 2015), and Brazil Current (Detoni et al., 2016). Furthermore, extremely high NFRs were detected in the waters (near the mainland) of western tropical South (570 μmol N m^{-2} d^{-1} on average with the highest up to 3,000 μmol N m^{-2} d^{-1}; Bonnet et al., 2017) and North (521 μmol N m^{-2} d^{-1}; Wen et al., 2022) Pacific, which originated from the South and North Equatorial Current, respectively. These regions appeared to provide optimal physicochemical conditions (particularly P and dFe) for transported diazotrophs (e.g., *Trichodesmium*) to bloom and N_2 fixation (Bonnet et al., 2017; Detoni et al., 2016; Jiang, Li, et al., 2018; Palter et al., 2020; Shiozaki, Takeda, et al., 2015). Therefore, we infer that the intrusion of western boundary currents (originated from equatorial currents) into marginal seas fuels regional N_2 fixation.

Our result revealed slightly higher NFR on the surface than at the 10% light depth (~5–45 m with 100–250 μmol quanta m^{-2} s^{-1}). This result was highly supported by the abundant filamentous diazotrophs in upper 45 m (Jiang et al., 2019) as well as their high adaptability to this relatively low light environment (Lu et al., 2018; Villareal, 1990). Previous studies also showed relatively low variability in NFRs throughout the euphotic zone, except for 1% of the surface irradiance, such as the ECS (Zhang et al., 2012) and Northwestern Atlantic Ocean (Capone et al., 2005). Additionally, unicellular diazotrophs fixed N_2 under low light and even night (Chen et al., 2014; Zehr et al., 2001), which smoothed this difference of NFR between light depths.

4.2. Influences of Large River Plume and Upwelling on N_2 Fixation

The CDW, dominates the northern ECS and the southern part of the SYS during summer, delivers a large amount of freshwater and associated macro- and micro-nutrients from the Changjiang. The low-salinity (≤31) and N-replete (high NO_3^-/DRP) conditions therein fueled nondiazotrophic phytoplankton growth but depressed filamentous diazotrophs and N_2 fixation (Figures 2–4). Table 2 showed that NFRs were significantly ($p < 0.01$) positively correlated with salinity but was negatively with NO_3^-, NO_3^-/DRP, and Chl-*a*. This result disagreed with previous studies in the plumes of Amazon (Subramaniam et al., 2008) and Mekong Rivers (Voss et al., 2006), which found abundant filamentous diazotrophs and active N_2 fixation. Particularly DDAs, were benefited from the nutrient environment (depleted N, available P and silicate, and abundant dFe) of the Amazon River plume (Carpenter et al., 1999; Subramaniam et al., 2008). We inferred that the differences of nutrient conditions and diazotrophic composition in plumes of Changjiang (higher N:P ratio, depleted silicate, and lower densities of DDAs and *Trichodesmium*) and Amazon River (lower N:P ratio, abundant silicate, and higher densities of DDAs and *Trichodesmium*) were the main reason.

Under the prevailing southwestern monsoon, the shoreward and northward intrusions of saline, cold deeper TWC and nearshore Kuroshio Branch Current onto the ECS shelf increased significantly during summer (Yang et al., 2012, 2018; Zhou et al., 2015), resulting in strong upwelling in the Zhejiang coastal waters and Changjiang

Estuary because of tidal mixing, topography, and winds (Lü et al., 2006). In this study, high salinity (>31–32; Figure 2a) and low temperature (<26–27°C; Figure 2b) were observed along the ECS coast and in the Changjiang Estuary. Moreover, this upwelling most likely mixed with eutrophic CDW and coastal water, resulting in low temperature (23.9 ± 1.8°C), abundant NO_3^- (12.61 ± 8.67 μmol L^{-1}), and high NO_3^-/DRP ratio (21.9 ± 16.9) on the surface (Table 1). Such an environment stimulated nondiazotrophic phytoplankton blooms (with Chl-*a* concentration at 6.34 ± 7.56 mg m^{-3}) but restrained growth of filamentous diazotrophs (Figure 3) and N_2 fixation (Figure 4). This finding was consistent with those reported in upwelling waters off Vietnam (Voss et al., 2006) and Hainan Island (Zhang, Chen et al., 2015) in the South China Sea, although higher NFRs occurred in bordering between coastal upwelled and offshore waters. However, our result differed from those reported in upwelling systems of the eastern equatorial Atlantic (Subramaniam et al., 2013) and off Pingtan in the Taiwan Strait (Wen et al., 2017). Subramaniam et al. (2013) hypothesized that upwelled low N:P ratio water and reduced N (because of initial bloom of nondiazotrophic phytoplankton) resulted in active N_2 fixation that fueled by residual P and a combination of aeolian and upwelled Fe. Wen et al. (2017) observed much higher surface NFR in upwelling region off Pingtan (up to 7.5 nmol N L^{-1} d^{-1} with low N:P ratio of 1.0–10.4) than off Dongshan (<1.9 nmol N L^{-1} d^{-1} with high N:P ratio up to 43 due to influence of the Pearl River plume) in the Taiwan Strait, which was highly attributed to N:P ratio. This observation supported our finding of extreme low NFR in the ECS coastal upwelling waters where was characterized by abundant NO_3^- and high NO_3^-/DRP ratio of 21.9 due to influence of the CDW and coastal water. The response mechanisms of diazotrophs and N_2 fixation to dynamic upwelling events are not uniform across coastal upwelling systems characterized by different physical and biogeochemical conditions, which warrants further study.

4.3. Biogeochemical Importance of Filamentous Diazotrophs and N_2 Fixation

The present study did not directly measure the contribution of filamentous and unicellular diazotrophs to the bulk NFR in the ECSYS using size-fractionated $^{15}N_2$ tracer assay. However, we estimated that the NFRs of *Trichodesmium* and *Richelia/Calothrix* in the ECS were at 48.3 and 9.4 μmol N m^{-2} d^{-1}, respectively, based on their DIDs in the euphotic zone (Jiang et al., 2019). This estimation adopted the summer NFRs of colonial *Trichodesmium* (7.9 pmol N $trichome^{-1}$ d^{-1}) measured in the ECS Kuroshio (Wu et al., 2018) and of *Richelia/Calothrix* (1.04, 0.55, and 0.51 pmol N $heterocyst^{-1}$ hr^{-1} for *Rhizosolenia*, *Hemiaulus*, and *Chaetoceros*, respectively) in the North Pacific (29.8°N, 149.3°E, near the Kuroshio Extension; Kitajima et al., 2009). Our assumption of the NFR of free trichomes (2.63 pmol N $trichome^{-1}$ d^{-1}) was lower than those reported in the ECS (5.6 pmol N $trichome^{-1}$ d^{-1}; Chang et al., 2000) and the western North Pacific (16.1 pmol N $trichome^{-1}$ d^{-1}; 32.0°N, 155.0°E) (Kitajima et al., 2009). Therefore, the present estimated NFR of *Trichodesmium* was quite conservatively. According to our measured NFR, the contribution of filamentous diazotrophs to N_2 fixation in the ECS was estimated to be 64%. Particularly in oceanic region, their contribution might frequently exceed 90% because of extremely abundant *Trichodesmium* (Jiang, Li, et al., 2018; Marumo & Asaoka, 1974; Shiozaki Takeda et al., 2015). This contribution in the ECS was comparable with that (59.1%) measured in the upstream Kuroshio but higher than that (39.5%) measured in the South China Sea during summer using a size-fractionated method (Chen et al., 2014). Because our estimation of *Trichodesmium* NFR was quite conservative, the actual NFR and contribution of filamentous diazotrophs might be much higher than these values. Regardless, our results showed a crucial role of filamentous diazotrophs in N_2 fixation in the ECS.

Summer *Trichodesmium* densities, both in the ECS and SYS, have evidently increased since the 1970s under increased temperature and enhanced northerly transport of the nearshore Kuroshio Branch Current (Jiang et al., 2017; Jiang, Li, et al., 2018), although the present density (4.6 ± 7.0 × 10^3 trichomes m^{-2}) of *Trichodesmium* in the SYS was lower than that (30 ± 53 × 10^3 trichomes m^{-2}) observed previously in summer 2011 (Jiang, Li, et al., 2018). The present stronger upwelling and CDW and associated abundant NO_3^- in the southern part of the SYS were largely responsible for this contradiction. Furthermore, the distribution boundary of *Trichodesmium* shifted northward in the ECSYS and high density (up to 5 × 10^6 trichomes m^{-2}) was found in the southern part of the SYS near the Changjiang Estuary in autumn with surface temperature of ∼22°C (Jiang, Li, et al., 2018). With increasing surface temperature and stratification, oligotrophic subtropical conditions were expected to extend to higher latitudes (Polovina et al., 2008). Correspondingly, *Trichodesmium* had the potential to shift poleward, resulting in increases of growth rate and NFR in subtropical waters within 30°C (Breitbarth et al., 2007). Laboratory experiments found that growth rate and NFR of *Trichodesmium* enhanced significantly under elevated pCO_2 (Hutchins et al., 2015). We speculated that contribution of *Trichodesmium* to N_2 fixation in the subtropical ECS and temperate SYS (N-limited in the central part because of strong thermocline) likely to be enhanced in warmer, more acidified environment.

As mentioned before, spatial pattern of NFR in the ECS was highly associated with the saline, oligotrophic Kuroshio intrusion. We divided the ECS into three regions, including oceanic (surface salinity ≥34), mesohaline (31 < surface salinity <34), and coastal regions (surface salinity ≤31; including upwelling). Then we calculated the areas of oceanic (207.13×10^3 km^2), mesohaline (293.09×10^3 km^2), and coastal (194.37×10^3 km^2) regions according to the salinity distribution (Figure 2a). Based on the present average NFRs (428.3, 47.8, and 4.7 μmol N m^{-2} d^{-1}, respectively) across oceanic, mesohaline, and coastal regions (Figure 4c), summer (June–August) N_2 fixation in the entire ECS (excluding the Taiwan Strait) was estimated to be approximately 0.13 Tg N. This flux was overwhelmingly contributed (85.6%) by the oceanic region, while the mesohaline and coastal regions accounted for 13.5% and 0.9%, respectively. Previous study in the *Trichodesmium*-dominant section 23°W (15°N–5°S) of the Atlantic Ocean suggested that average depth-integrated NFR was 62% higher with the dissolution method than with the original bubble method (Großkopf et al., 2012). If we accept this correction coefficient, the estimated N_2 fixation was 0.22 Tg N. This estimation of pelagic fixed N was accounted for >40% of the summer (June–August) NO_3^- flux (0.49 Tg N) from Changjiang calculated through monthly river inflow and NO_3^- concentration (see data set) at station Datong during 2017–2019. The summer N_2 fixation flux was accounted for 13% of the annual dissolved inorganic N flux (115×10^9 mol) of Changjiang estimated using nutrient data from the river mouth during 2004–2015 (Zhang et al., 2020). Additionally, the present NFRs in the ECS oceanic and mesohaline regions were comparable with vertical turbulent NO_3^- fluxes in the Kuroshio mainstream (445 μmol N m^{-2} d^{-1}) and outer shelf (82 μmol N m^{-2} d^{-1}) of the ECS, respectively (Liu et al., 2013), indicating that N_2 fixation was a major new N source in the ECS open waters. Therefore, our study suggested that N_2 fixation is an important external source of N budget in the ECS.

New production across the ECS during summer 2011 was 9.8 ± 6.4 ($n = 9$) mmol C m^{-2} d^{-1} measured using ^{15}N ($K^{15}NO_3$) tracing method (see data set). Assuming that the NFR was converted to C fixation using a C:N ratio at 6.6 (Redfield, 1958), diazotrophs roughly contributed 6.1% to new production across the ECS. However, the contribution was up to 55.8% in the Kuroshio mainstream. This contribution was higher than those estimated in the upstream Kuroshio (16%; Chen et al., 2008) and the ECS outer shelf (17%) and Kuroshio (10%; Liu et al., 2013) but lower than in south of the Ryukyu Island Chain (82%; Liu et al., 2013). Our result suggested that N_2 fixation played an important role in C fixation in the ECS, particularly in the Kuroshio, which enhanced sequestration of CO_2 (Falkowski, 1997; Subramaniam et al., 2008). We inferred that the contribution of *Richelia/Calothrix* to new production was lower than that of *Trichodesmium* in the ECS because of their varying standing crop and estimated NFR. Nevertheless, *Richelia/Calothrix* with heavy, silicon-containing cell walls might fuel more efficient CO_2 sequestration and enhance efficiency of the biological C pump in the Kuroshio. Sediment trap data confirmed that N_2 fixation by DDAs contributed significantly to particulate C sink in the North Pacific subtropical gyre (Karl et al., 2012), tropical North Atlantic (Subramaniam et al., 2008), and Gulf of California (White et al., 2013). These results warrant further study on new production and C sequestration sustained by filamentous diazotrophs in the Kuroshio and affected waters.

5. Conclusions

We found active N_2 fixation in oceanic and mesohaline waters of the ECS influenced by the Kuroshio, which was significantly contributed by filamentous diazotrophs (*Trichodesmium* and *Richelia/Calothrix*). These results confirmed our hypothesis that the intrusion of Kuroshio greatly enhanced N_2 fixation in the ECSYS. Based on the present finding in the Kuroshio and recent evidence in the Gulf Stream (Palter et al., 2020), Brazil Current (Detoni et al., 2016, 2022) and East Australian Current (Armbrecht et al., 2015), we infer that the intrusion of western boundary currents into marginal seas fuels regional N_2 fixation. Our study provided high spatial resolution data sets of NFR in the ECSYS during summer, which would be useful for understanding N and C biogeochemical process, although the present use of original bubble method might underestimate the NFR. We estimated the contribution of filamentous diazotrophs to N_2 fixation based on reported NFR per trichome or heterocyst, further study on size-fractionated NFR using $^{15}N_2$ dissolution method or modified bubble method needs to be performed to more accurately calculate their contribution and regional budget of N_2 fixation. Moreover, our study highlights an appreciable contribution of summer N_2 fixation to N budget in the ECS, which warrants further direct measurement of NFRs in different seasons.

Conflict of Interest

The authors declare no conflicts of interest relevant to this study.

Data Availability Statement

Data set for this paper are freely available online through Figshare (http://dx.doi.org/10.6084/m9.figshare.20045705).

Acronyms

C	carbon
CDW	Changjiang Diluted Water
Chl-*a*	chlorophyll *a*
DDA	diatom-diazotroph associations
DID	depth-integrated density
dFe	dissolved iron
ECS	East China Sea
ECSYS	East China Sea and southern Yellow Sea
MLD	mixed layer depth
NFR	N_2 fixation rate
N	nitrogen
P	phosphorus
SYS	southern Yellow Sea
TWC	Taiwan Warm Current

Acknowledgments
We are grateful to Prof. Wensheng Jiang for providing the data of temperature, salinity, and turbidity in July 2013. We also thank the Associate editor and anonymous reviewers for their constructive comments. This work was funded by the National Natural Science Foundation of China (41876198 and 42076134), Scientific Research Fund of the Second Institute of Oceanograph, MNR (JG2311), Zhejiang Provincial Natural Science Foundation of China (LR22D060001), National Key Research and Development Program of China (2021YFC3101702), Key R&D Program of Zhejiang (2022C03044), National Basic Research Program of China (2010CB428903 and 2011CB409803), and Project of Long-term Observation and Research Plan in the Changjiang Estuary and Adjacent East China Sea (LORCE; SZ2001).

References

Armbrecht, L. H., Schaeffer, A., Roughan, M., & Armand, L. K. (2015). Interactions between seasonality and oceanic forcing drive the phytoplankton variability in the tropical-temperate transition zone (~30°S) of Eastern Australia. *Journal of Marine Systems*, *144*, 92–106. https://doi.org/10.1016/j.jmarsys.2014.11.008

Bonnet, S., Caffin, M., Berthelot, H., & Moutin, T. (2017). Hot spot of N_2 fixation in the western tropical South Pacific pleads for a spatial decoupling between N_2 fixation and denitrification. *Proceedings of the National Academy of Sciences of the USA*, *114*(14), E2800. https://doi.org/10.1073/pnas.1619514114

Breitbarth, E., Oschlies, A., & LaRoche, J. (2007). Physiological constraints on the global distribution of *Trichodesmium*–effect of temperature on diazotrophy. *Biogeosciences*, *4*(1), 53–61. https://doi.org/10.5194/bg-4-53-2007

Capone, D. G., Bronk, D. A., Mulholland, M. R., & Carpenter, E. J. (2008). *Nitrogen in the marine environment*. Academic Press.

Capone, D. G., Burns, J. A., Montoya, J. P., Subramaniam, A., Mahaffey, C., Gunderson, T., et al. (2005). Nitrogen fixation by *Trichodesmium* spp.: An important source of new nitrogen to the tropical and subtropical North Atlantic Ocean. *Global Biogeochemical Cycles*, *19*(2), GB2024. https://doi.org/10.1029/2004GB002331

Capone, D. G., Zehr, J. P., Pearl, H. W., Bergman, B., & Carpenter, E. J. (1997). *Trichodesmium*, a globally significant marine cyanobacterium. *Science*, *276*(5316), 1221–1229. https://doi.org/10.1126/science.276.5316.1221

Carpenter, E. J., Montoya, J. P., Mulholland, M. R., Subramaniam, A., & Capone, D. G. (1999). Extensive bloom of a N_2 fixing diatom/cyanobacterial association in the tropical Atlantic Ocean. *Marine Ecology Progress Series*, *185*, 273–283. https://doi.org/10.3354/meps185273

Chang, J., Chiang, K. P., & Gong, G. C. (2000). Seasonal variation and cross-shelf distribution of the nitrogen-fixing cyanobacterium, *Trichodesmium*, in southern East China Sea. *Continental Shelf Research*, *20*(4–5), 479–492. https://doi.org/10.1016/S0278-4343(99)00082-5

Chen, C. T. A. (2009). Chemical and physical fronts in the Bohai, Yellow and East China seas. *Journal of Marine Systems*, *78*(3), 394–410. https://doi.org/10.1016/j.jmarsys.2008.11.016

Chen, Y. L. L., Chen, H. Y., Lin, Y. H., Yong, T. C., Taniuchi, Y., & Tuo, S. (2014). The relative contributions of unicellular and filamentous diazotrophs to N_2 fixation in the South China Sea and the upstream Kuroshio. *Deep Sea Research Part I: Oceanographic Research Papers*, *85*, 56–71. https://doi.org/10.1016/j.dsr.2013.11.006

Chen, Y. L. L., Chen, H. Y., Tuo, S. H., & Ohki, K. (2008). Seasonal dynamics of new production from *Trichodesmium* N_2 fixation and nitrate uptake in the upstream Kuroshio and South China Sea basin. *Limnology and Oceanography*, *53*(5), 1705–1721. https://doi.org/10.4319/lo.2008.53.5.1705

Cheung, S., Suzuki, K., Xia, X., & Liu, H. (2019). Transportation of diazotroph community from the upstream to downstream of the Kuroshio. *Journal of Geophyscial Research: Biogeosciences*, *124*(9), 2680–2693. https://doi.org/10.1029/2018JG004960

Detoni, A. M. S., Ciotti, Á. M., Calil, P. H. R., Tavano, V. M., & Yunes, J. S. (2016). *Trichodesmium* latitudinal distribution on the shelf break in the southwestern Atlantic Ocean during spring and autumn. *Global Biogeochemical Cycles*, *30*(11), 1738–1753. https://doi.org/10.1002/2016GB005431

Detoni, A. M. S., Subramaniam, A., Haley, S. T., Dyhrman, S. T., & Calil, P. H. R. (2022). Cyanobacterial diazotroph distributions in the Western South Atlantic. *Frontiers in Marine Science*, *9*, 856643. https://doi.org/10.3389/fmars.2022.856643

Dugdale, R. C., & Goering, J. J. (1967). Uptake of new and regenerated forms of nitrogen in primary productivity. *Limnology and Oceanography*, *12*(2), 196–206. https://doi.org/10.4319/lo.1967.12.2.0196

Falkowski, P. G. (1997). Evolution of the nitrogen cycle and its influence on the biological sequestration of CO_2 in the ocean. *Nature*, *387*(6630), 272–275. https://doi.org/10.1038/387272a0

Fu, F. X., & Bell, P. R. F. (2003). Effect of salinity on growth, pigmentation, N_2-fixation and alkaline phosphatase activity of cultured *Trichodesmium* sp. *Marine Ecology Progress Series*, *257*, 69–76. https://doi.org/10.3354/meps257069

Großkopf, T., Mohr, W., Baustian, T., Schunck, H., Gill, D., Kuypers, M. M. M., et al. (2012). Doubling of marine dinitrogen-fixation rate based on direct measurements. *Nature*, *488*(7411), 361–364. https://doi.org/10.1038/nature11338

Guo, L., Chen, Y., Wang, F., Meng, X., Xu, Z., & Zhuang, G. (2014). Effects of Asian dust on the atmospheric input of trace elements to the East China Sea. *Marine Chemistry*, *163*, 19–27. https://doi.org/10.1016/j.marchem.2014.04.003

Huang, R. X., & Russell, S. (1994). Ventilation of the subtropical North Pacific. *Journal of Physical Oceanography*, *24*(12), 2589–2605. https://doi.org/10.1175/1520-0485(1994)024<2589:votsnp>2.0.co;2

Hutchins, D. A., Walworth, N. G., Webb, E. A., Saito, M. A., Moran, D., McIlvin, M. R., et al. (2015). Irreversibly increased nitrogen fixation in *Trichodesmium* experimentally adapted to elevated carbon dioxide. *Nature Communications*, *6*(1), 8155. https://doi.org/10.1038/ncomms9155

Jiang, H.-B., Fu, F.-X., Sara, R. C., Levine, N. M., Sañudo-Wilhelmy, S. A., Qu, P.-P., et al. (2018). Ocean warming alleviates iron limitation of marine nitrogen fixation. *Nature Climate Change*, *8*, 709–712. https://doi.org/10.1038/s41558-018-0216-8

Jiang, Z., Chen, J., Zhai, H., Zhou, F., Yan, X., Zhu, Y., et al. (2019). Kuroshio shape composition and distribution of filamentous diazotrophs in the East China Sea and southern Yellow Sea. *Journal of Geophyscial Research: Oceans*, *124*(11), 7421–7436. https://doi.org/10.1029/2019JC015413

Jiang, Z., Chen, J., Zhou, F., Zhai, H., Zhang, D., & Yan, X. (2017). Summer distribution patterns of *Trichodesmium* spp. in the Changjiang (Yangtze River) estuary and Adjacent East China Sea shelf. *Oceanologia*, *59*(3), 248–261. https://doi.org/10.1016/j.oceano.2017.02.001

Jiang, Z., Li, H., Zhai, H., Zhou, F., Chen, Q., Chen, J., et al. (2018). Seasonal and spatial changes in *Trichodesmium* associated with physicochemical properties in East China Sea and southern Yellow Sea. *Journal of Geophyscial Research: Biogeosciences*, *123*(2), 509–530. https://doi.org/10.1002/2017JG004275

Jiao, N. (2021). Developing ocean negative carbon emission technology to support national carbon neutralization. *Bulletin of Chinese Academy of Sciences*, *36*, 179–187. https://doi.org/10.16418/j.issn.1000-3045.20210123001

Jickells, T. D., An, Z. S., Andersen, K. K., Baker, A. R., Bergametti, G., Brooks, N., et al. (2005). Global iron connections between desert dust, ocean biogeochemistry, and climate. *Science*, *308*(5718), 67–71. https://doi.org/10.1126/science.1105959

Karl, D. M., Church, M. J., Dore, J. E., Letelier, R. M., & Mahaffey, C. (2012). Predictable and efficient carbon sequestration in the North Pacific Ocean supported by symbiotic nitrogen fixation. *Proceedings of the National Academy of Sciences of the USA*, *109*(6), 1842–1849. https://doi.org/10.1073/pnas.1120312109

Kitajima, S., Furuya, K., Hashihama, F., Takeda, S., & Kanda, J. (2009). Latitudinal distribution of diazotrophs and their nitrogen fixation in the tropical and subtropical Western North Pacific. *Limnology and Oceanography*, *54*(2), 537–547. https://doi.org/10.4319/lo.2009.54.2.0537

Letelier, R. M., & Karl, D. M. (1998). *Trichodesmium* spp. physiology and nutrient fluxes in the North Pacific subtropical gyre. *Aquatic Microbial Ecology*, *15*, 265–276. https://doi.org/10.3354/ame015265

Liu, X., Furuya, K., Shiozaki, T., Masuda, T., Kodama, T., Sato, M., et al. (2013). Variability in nitrogen sources for new production in the vicinity of the shelf edge of the East China Sea in summer. *Continental Shelf Research*, *61–62*, 23–30. https://doi.org/10.1016/j.csr.2013.04.014

Lü, X., Qiao, F., Xia, C., Zhu, J., & Yuan, Y. (2006). Upwelling off Yangtze River estuary in summer. *Journal of Geophysical Research*, *111*(C11), C11S08. https://doi.org/10.1029/2005JC003250

Lu, Y., Wen, Z., Shi, D., Chen, M., Zhang, Y., Bonnet, S., et al. (2018). Effect of light on N_2 fixation and net nitrogen release of *Trichodesmium* in a field study. *Biogeosciences*, *15*(1), 1–12. https://doi.org/10.5194/bg-15-1-2018

Lu, Y., Wen, Z., Shi, D., Lin, W., Bonnet, S., Dai, M., & Kao, S. J. (2019). Biogeography of N_2 fixation influenced by the western boundary current intrusion in the South China Sea. *Journal of Geophysical Research: Oceans*, *124*(10), 6983–6996. https://doi.org/10.1029/2018JC014781

Luo, Y., Doney, S. C., Anderson, L. A., Benavides, M., Berman-Frank, I., Bode, A., et al. (2012). Database of diazotrophs in global ocean: Abundance, biomass and nitrogen fixation rates. *Earth System Science Data*, *4*(1), 47–73. https://doi.org/10.5194/essd-4-47-2012

Martiny, A. C., Lomas, M. W., Fu, W., Boyd, P. W., Chen, Y. L. L., Cutter, G. A., et al. (2019). Biogeochemical controls of surface ocean phosphate. *Science Advances*, *5*(8), eaax0341. https://doi.org/10.1126/sciadv.aax0341

Marumo, R., & Asaoka, O. (1974). *Trichodesmium* in the East China Sea. 1. Distribution of *Trichodesmium thiebautii* Gomont during 1961–1967. *Journal of the Oceanographical Society of Japan*, *30*, 48–53.

Mills, M. M., Ridame, C., Davey, M., LaRoche, J., & Gelder, R. J. (2004). Iron and phosphorus co-limit nitrogen fixation in the eastern tropical North Atlantic. *Nature*, *429*(6989), 292–294. https://doi.org/10.1038/nature02550

Mohr, W., Großkopf, T., Wallace, D. W. R., & LaRoche, J. (2010). Methodological underestimation of oceanic nitrogen fixation rates. *PLoS One*, *5*(9), e12583. https://doi.org/10.1371/journal.pone.0012583

Montoya, J. P., Voss, M., Kahler, P., & Capone, D. G. (1996). A simple, high-precision, high-sensitivity tracer assay for N_2 fixation. *Applied and Environmental Microbiology*, *62*(3), 986–993. https://doi.org/10.1128/aem.62.3.986-993.1996

Moore, C. M., Mills, M. M., Arrigo, K. R., Berman-Frank, I., Bopp, L., Boyd, P. W., et al. (2013). Processes and patterns of oceanic nutrient limitation. *Nature Geoscience*, *6*(9), 701–710. https://doi.org/10.1038/ngeo1765

Palter, J. B., Ames, E. J., Benavides, M., Neto, G. A., Granger, J., Moisander, P. H., et al. (2020). High N_2 fixation in and near the Gulf Stream consistent with a circulation control on diazotrophy. *Geophysical Research Letters*, *47*(16). https://doi.org/10.1029/2020GL089103

Polovina, J. J., Howell, E. A., & Abecassis, M. (2008). Ocean's least productive waters are expanding. *Geophysical Research Letters*, *35*(3), L03618. https://doi.org/10.1029/2007GL031745

Redfield, A. C. (1958). The biological control of chemical factors in the environment. *American Scientist*, *46*, 205–221.

Saino, T., & Hattori, A. (1982). Aerobic nitrogen fixation by the marine non-heterocystous cyanobacterium *Trichodesmium* (*Oscillatoria*) spp.: Its protective mechanism against oxygen. *Marine Biology*, *70*(3), 72–76. https://doi.org/10.1007/BF00396843

Sato, M., Nishioka, J., Maki, K., & Takeda, S. (2021). Chemical speciation of iron in the euphotic zone along the Kuroshio Current. *Marine Chemistry*, *233*, 103966. https://doi.org/10.1016/j.marchem.2021.103966

Shiozaki, T., Furuya, K., Kodama, T., Kitajima, S., Takeda, S., Takemura, T., & Kanda, J. (2010). New estimation of N_2 fixation in the western and central Pacific Ocean and its marginal seas. *Global Biogeochemical Cycles*, *24*(1), GB1015. https://doi.org/10.1029/2009GB003620

Shiozaki, T., Kodama, T., & Furuya, K. (2014). Large-scale impact of the island mass effect through nitrogen fixation in the western South Pacific Ocean. *Geophysical Research Letters*, *41*(8), 2907–2913. https://doi.org/10.1002/2014GL059835

Shiozaki, T., Kondo, Y., Yuasa, D., & Takeda, S. (2018). Distribution of major diazotrophs in the surface water of the Kuroshio from northeastern Taiwan to south of mainland Japan. *Journal of Plankton Research*, *40*(4), 407–419. https://doi.org/10.1093/plankt/fby027

Shiozaki, T., Nagata, T., Ijichi, M., & Furuya, K. (2015). Nitrogen fixation and the diazotroph community in the temperate coastal region of the northwestern North Pacific. *Biogeosciences*, *12*(15), 4751–4764. https://doi.org/10.5194/bg-12-4751-2015

Shiozaki, T., Takeda, S., Itoh, S., Kodama, T., Liu, X., Hashihama, F., & Furuya, K. (2015). Why is *Trichodesmium* abundant in the Kuroshio? *Biogeosciences*, *12*(23), 693–6943. https://doi.org/10.5194/bg-12-6931-2015

Sohm, J. A., Webb, E. A., & Capone, D. G. (2011). Emerging patterns of marine nitrogen fixation. *Nature Reviews Microbiology*, *9*(7), 499–508. https://doi.org/10.1038/nrmicro2594

Su, J., & Yuan, Y. (2005). *Hydrology in China Sea (in Chinese)*. Ocean Press.

Subramaniam, A., Mahaffey, C., Johns, W., & Mahowald, N. (2013). Equatorial upwelling enhances nitrogen fixation in the Atlantic Ocean. *Geophysical Research Letters*, *40*(9), 1766–1771. https://doi.org/10.1002/grl.50250

Subramaniam, A., Yager, P. L., Carpenter, E. J., Mahaffey, C., Björkman, K., Cooley, S., et al. (2008). Amazon River enhances diazotrophy and carbon sequestration in the tropical North Atlantic Ocean. *Proceedings of the National Academy of Sciences of the USA*, *105*(30), 10460–10465. https://doi.org/10.1073/pnas.0710279105

Tang, W., Wang, S., Fonseca-Batista, D., Dehairs, F., Gifford, S., Gonzalez, A. G., et al. (2019). Revisiting the distribution of oceanic N_2 fixation and estimating diazotrophic contribution to marine production. *Nature Communications*, *10*(1), 831. https://doi.org/10.1038/s41467-019-08640-0

Tanita, I., Shiozaki, T., Kodama, T., Hashihama, F., Sato, M., Takahashi, K., & Furuya, K. (2021). Regionally variable responses of nitrogen fixation to iron and phosphorus enrichment in the Pacific Ocean. *Journal of Geophysical Research: Biogeosciences*, *126*(9), e2021JG006542. https://doi.org/10.1029/2021JG006542

Tyrrell, T. (1999). The relative influences of nitrogen and phosphorus on oceanic primary production. *Nature*, *400*(6744), 525–531. https://doi.org/10.1038/22941

Villareal, T. A. (1990). Laboratory culture and preliminary characterization of the nitrogen-fixing *Rhizosolenia-Richelia* symbiosis. *Marine Ecology*, *11*(2), 117–132. https://doi.org/10.1111/j.1439-0485.1990.tb00233.x

Voss, M., Bombar, D., Loick, N., & Dippner, J. W. (2006). Riverine influence on nitrogen fixation in the upwelling region off Vietnam, South China Sea. *Geophysical Research Letters*, *33*(7), L07604. https://doi.org/10.1029/2005GL025569

Wen, Z., Browning, T. J., Cai, Y., Dai, R., Zhang, R., Du, C., et al. (2022). Nutrient regulation of biological nitrogen fixation across the tropical Western North Pacific. *Science Advances*, *8*(5), eabl7564. https://doi.org/10.1126/sciadv.abl7564

Wen, Z., Lin, W., Shen, R., Hong, H., Kao, S. J., & Shi, D. (2017). Nitrogen fixation in two coastal upwelling regions of the Taiwan Strait. *Scientific Reports*, *7*(1), 17061. https://doi.org/10.1038/s41598-017-18006-5

White, A. E., Foster, R. A., Benitez-Nelson, C. R., Masqué, P., Verdeny, E., Popp, B. N., et al. (2013). Nitrogen fixation in the Gulf of California and the eastern tropical North Pacific. *Progress in Oceanography*, *109*(1), 1–17. https://doi.org/10.1016/j.pocean.2012.09.002

Wu, C., Fu, F. X., Sun, J., Thangaraj, S., & Pujari, L. (2018). Nitrogen fixation by *Trichodesmium* and unicellular diazotrophs in the northern South China Sea and the Kuroshio in summer. *Scientific Reports*, *8*(1), 2415. https://doi.org/10.1038/s41598-018-20743-0

Yang, D., Yin, B., Chai, F., Feng, X., Xue, H., Gao, G., & Yu, F. (2018). The onshore intrusion of Kuroshio subsurface water from February to July and a mechanism for the intrusion variation. *Progress in Oceanography*, *167*, 97–115. https://doi.org/10.1016/j.pocean.2018.08.004

Yang, D., Yin, B., Hou, Y., Sun, S., Yu, Z. M., Song, J. M., et al. (2017). Advance in research on Kuroshio intrusion and its ecological influence on the continental shelf of East China Sea. *Oceanologia et Limnologia Sinica*, *48*(6), 1196–1207. https://doi.org/10.11693/hyhz20170900223

Yang, D., Yin, B., Liu, Z., Bai, T., Qi, J., & Chen, H. (2012). Numerical study on the pattern and origins of Kuroshio branches in the bottom water of southern East China Sea in summer. *Journal of Geophysical Research*, *117*(C2), C02014. https://doi.org/10.1029/2011JC007528

Zehr, J. P., & Capone, D. G. (2020). Changing perspectives in marine nitrogen fixation. *Science*, *368*(6492), eaay9514. https://doi.org/10.1126/science.aay9514

Zehr, J. P., Waterbury, J. B., Turner, P. J., Montoya, J. P., Omoregie, E., Steward, G. F., et al. (2001). Unicellular cyanobacteria fix N_2 in the subtropical North Pacific Ocean. *Nature*, *412*(6847), 635–638. https://doi.org/10.1038/35088063

Zhang, J., Du, Y., Zhang, G., Chang, Y., Liu, S., Zhang, Z. F., et al. (2020). Increases in the seaward river flux of nutrients driven by human migration and land-use changes in the tide-influenced delta. *Science of The Total Environment*, *761*, 144501. https://doi.org/10.1016/j.scitotenv.2020.144501

Zhang, J., Zhu, X., Zhang, R., Ren, J., Wu, Y., Liu, S., & Huang, D. (2022). Dissolved Fe in the East China Sea under the influences of land sources and the boundary current with implications for global marginal seas. *Global Biogeochemical Cycles*, *36*(2), e2021GB006946. https://doi.org/10.1029/2021GB006946

Zhang, R., Chen, M., Cao, J., Ma, Q., Yang, J., & Qiu, Y. (2012). Nitrogen fixation in the East China Sea and southern Yellow Sea during summer 2006. *Marine Ecology Progress Series*, *447*, 77–86. https://doi.org/10.3354/meps09509

Zhang, R., Chen, M., Yang, Q., Lin, Y., Mao, H., Qiu, Y., et al. (2015). Physical-biological coupling of N_2 fixation in the northwestern South China Sea coastal upwelling during summer. *Limnology and Oceanography*, *60*(4), 1411–1425. https://doi.org/10.1002/lno.10111

Zhang, R., Zhang, D., Chen, M., Jiang, Z., Wang, C., Zheng, M., et al. (2019). N_2 fixation rate and diazotroph community structure in the Western tropical North Pacific Ocean (WTNP). *Acta Oceanologica Sinica*, *38*(12), 26–34. https://doi.org/10.1007/s13131-019-1513-4

Zhang, X., Song, Y., Liu, D., Keesing, J. K., & Gong, J. (2015). Macroalgal blooms favor heterotrophic diazotrophic bacteria in nitrogen-rich and phosphorus-limited coastal surface waters in the Yellow Sea. *Estuarine, Coastal and Shelf Sciece*, *163*, 75–81. https://doi.org/10.1016/j.ecss.2014.12.015

Zhou, F., Xue, H., Huang, D., Xuan, J., Ni, X., Xiu, P., & Hao, Q. (2015). Cross-shelf exchange in the shelf of the East China Sea. *Journal of Geophysical Research: Oceans*, *120*(3), 1545–1572. https://doi.org/10.1002/2014JC010567